

Buckling analysis of graphene oxide powder-reinforced nanocomposite beams subjected to non-uniform magnetic field

Farzad Ebrahimi*¹, Mostafa Nouraei¹, Ali Dabbagh² and Ömer Civalek³

¹Department of Mechanical Engineering, Faculty of Engineering, Imam Khomeini International University, Qazvin, Iran

²School of Mechanical Engineering, College of Engineering, University of Tehran, Tehran, Iran

³Akdeniz University, Engineering Faculty, Civil Engineering Dept., Division of Mechanics, 07058 Antalya, Turkey

(Received February 28, 2019, Revised April 1, 2019, Accepted April 5, 2019)

Abstract. Present article deals with the static stability analysis of compositionally graded nanocomposite beams reinforced with graphene oxide powder (GOP) is undertaken once the beam is subjected to an induced force caused by nonuniform magnetic field. The homogenized material properties of the constituent material are approximated through Halpin-Tsai micromechanical scheme. Three distribution types of GOPs are considered, namely uniform, X and O. Also, a higher-order refined beam model is incorporated with the dynamic form of the virtual work's principle to derive the partial differential motion equations of the problem. The governing equations are solved via Galerkin's method. The introduced mathematical model is numerically validated presenting a comparison between the results of present work with responses obtained from previous articles. New results for the buckling load of GOP reinforced nanocomposites are presented regarding for different values of magnetic field intensity. Besides, other investigations are performed to show the impacts of other variants, such as slenderness ratio, boundary condition, distribution type and so on, on the critical stability limit of beams made from nanocomposites.

Keywords: buckling; graphene oxide powder; refined higher-order beam theory; non-uniform magnetic field

1. Introduction

As time passes, the importance of using composite materials is becoming more and more obvious due to their various applications in many engineering fields of interest like civil, mechanical, marine and aeronautic. The composites are majorly chosen for their low weight to strength ratio. Composite materials are typically categorized with respect to their matrix constituent and their reinforcements. Fiber reinforced composite is one of the composite types which is composed of a group of fibers scattered in the matrix material. Because of their remarkable specific strength, specific stiffness and high resistance to fatigue failure, many models are allocated to analyze the mechanical performance of fiber reinforced composites. For example, Kant and Babu (2000) surveyed the buckling behaviors of skew composites reinforced with fibers under thermal loading via a shear deformable model coupled with the finite element method (FEM). Anlas and Göker (2001) investigated the vibration analysis of a laminated composite structure in which each layer was in a shape of skew plate and reinforced with fibers in order to find out how skew angle can affect the natural frequency of this structure. In other researches, a combination of both analytical and experimental methods is utilized to study the buckling behavior of both cantilever I and open channel beams by considering shear effects (Shan and Qiao, 2005).

Laminated composites (LCs) are made from of a series of layers held together by matrix. Sandwich structures can be categorized in this group of composites. The layers are often of different materials, but not necessary. Laminates are also able to provide a group of needed engineering features, like in-plane stiffness, bending stiffness, strength, and thermal expansion coefficient. According to these properties of laminated composites and their potential to be used in evolving applications, scientists have tried to analyze these materials as more as possible recently. Liu *et al.* (2002) presented an investigation on the buckling analysis of LC plates via an element-free Galerkin method to show the efficiency of this method. Afterwards, A global higher-order plate theory was presented by Zhen and Wanji (2006) to probe the free vibration problem of LC plates. Urthaler and Reddy (2008) investigated the bending response of LC plates to find out an accurate prediction of the global bending response of the plates with different thickness subjected to large rotation. Shariyat (2010) introduced a new theory for analyzing the thermally affected bending and vibrational behavior of sandwich plates to cover the continuity conditions between layers. Also, some investigations have been performed on LCs via non-uniform rational B-splines (NURBS) method (Shojaee *et al.* 2012). Carrera Unified Formulation (CUF) was employed by Tornabene *et al.* (2014) in order to analyze the stability problem of doubly-curved shells. The Fourier-Ritz method was applied by Wang *et al.* (2017) with the aim of analyzing the vibrational behavior of LC shells and panels by considering various boundary conditions (BCs). Sobhani *et al.* (2018) solved the stability problem of LC with respect to the delamination effects in the framework of acoustic

*Corresponding author, Professor
E-mail: febrahimi@eng.ikiu.ac.ir

emission and signal processing techniques. Pandey and Sharma (2018) reviewed the ecological friendly functional fluids and lubricant techniques in machining processes and the applications of shear thickening fluids was presented by Tian *et al.* (2018). Micro and nanostructures have been introduced as novel materials whose size of elemental structure has been engineered at the micro or nanometer scale. The curiosity of the researchers has been driven into nanostructures due to the novel applications of these structures in almost all branches of technology. For instant, the dynamic and static behaviors of some microstructures have been analyzed recently to show hoe these structures can be applicable for engineering purposes (Akgoz and Civalek, 2013). Some mechanical responses of the nanobeams have been investigated by Bellifa *et al.* (2017) on the basis of nonlocal shear deformation theory. Several effects such as thermal loadings, elastic foundations and magnetic field are applied to the nanostructures like nanobeams and nanoplates by the researchers (Hamza-Cherif *et al.* 2018, Ebrahimi and Barati, 2016a-n; Ebrahimi *et al.* 2016a; Ebrahimi and Dabbagh; 2016; Ebrahimi and Hosseini; 2016a, b) in order to find out how these effects can influence the buckling and vibrational responses of these nanostructures.

Also the wave propagation, buckling and bending analysis of the nanotubes have been carried out She *et al.* (2018b). The application of the nonlocal strain gradient theory in the wave propagation analysis of the porous nanobeams presented by She *et al.* (2018a). The wave propagation analysis of the nanoshells and magneto-electro-elastic (MEE) nanotubes have been investigated by Ebrahimi *et al.* (2019) based on the nonlocal strain gradient elasticity theory. In addition, the wave dispersion analysis of the rotating FG nanobeams have been conducted by the same authors (Ebrahimi *et al.* 2018, Ebrahimi and Haghi, 2018) by utilizing nonlocal elasticity theory. The nonlinear bending responses of the curved nanotubes have been performed by She *et al.* (2019) for the first time by implementing nonlocal strain grading theory to describe the stiffness enhancement and stiffness reduction effects.

Furthermore, once elements with at least one dimension in nano scale are selected as reinforcements, the composite is named a nanocomposite. Indeed, the outstanding mechanical properties of nanoparticles were appealing enough in the engineers' opinion to be employed as reinforcement in composites. One of the most famous nano size reinforcing elements is carbon nanotube (CNT) which is an important new class of technological materials that possesses numerous novel and useful properties. Therefore, it is of high importance to analyze the mechanical behaviors of CNT reinforced (CNTR) nanocomposites. In a remarkable endeavor, the Eshelby-Mori-Tanaka homogenization model was employed by Formica *et al.* (2010) to investigate the vibration behavior of CNTR nanocomposites via FEM. Single-walled CNTs (SWCNTs) have attracted the attention of the researchers recently with their evolving applications such as reinforcements in composites, additives in polymers, catalysts and so on. For example, Shen and Zhang (2010) investigated both thermo-elastic pre- and post-buckling response of nanocomposite plates reinforced with SWCNTs to show how the

nanofillers' distribution type can improve the stability limits of nanocomposite plates. Also, Arani *et al.* (2011) employed both FE and analytical methods to investigate effects of some variants such as aspect ratio, BCs and CNTs' orientation on the buckling loads of SWCNT reinforced LC plates. Wang and Shen (2011) presented a thermal analysis on the nonlinear vibrational behaviors of nanocomposite plates reinforced with SWCNTs via a higher-order plate theory. Both static and dynamic FEM analyses of SWCNT reinforced nanocomposite plates have been performed by Zhu *et al.* (2012) by considering different types of reinforcements' distributions. In addition, Shen and Xiang (2012) probed the nonlinear thermal vibration behaviors of CNTR nanocomposite shells with respect to various distribution patterns of nanofillers. Yas and Samadi (2012) solved the vibration and buckling problems of the CNTR nanocomposite beams numerically by considering the influences of elastic foundation. Moreover, Wattanasakulpong and Ungbhakorn (2013) surveyed bending, buckling and vibration behaviors of the embedded nanocomposite beams reinforced with SWCNTs by the means of Navier method. Lei *et al.* (2013) implemented the Eshelby-Mori-Tanaka homogenization technique to account for the nanotubes' aggregation while investigating the buckling behaviors of CNTR nanocomposite plates via a FE based element-free method. In another research, Liew *et al.* (2014) introduced a meshless approach for the purpose of studying the post-buckling responses of axially compressed CNTR nanocomposite panels. Also, Zhang *et al.* (2015) employed first-order shear deformation plate theory incorporated with Ritz method to analyze the vibrational behaviors of CNTR skew nanocomposites. Wu *et al.* (2016) found it significant to account for the geometrical imperfections once examining the nonlinear vibration behaviors of FG-CNTR nanocomposite beams. Ebrahimi and Farazmandnia (2017) employed a higher-order shear deformation beam theory to analyze the thermo-mechanical vibration of sandwich beams with FG-CNTR nanocomposite face sheets. Ebrahimi and Rostami (2018) have just analyzed the wave propagation problem of CNTR nanocomposite beams via different shear deformation theories.

On the other hand, CNTs are not the only nano size reinforcement which is used in the nanocomposites. Nano fillers consisted of other carbon-based materials are utilized in nanocomposites, too. For instant, graphene platelets (GPLs) and graphene oxide powders (GOPs) are recently employed by researchers to design and analyze novel nanocomposites. Suk *et al.* (2010) investigated the mechanical properties of the GO by combining the AFM measurement with the FEM in a new approach for evaluating the mechanical properties of ultrathin membranes. The Halpin-Tsai model was employed by Feng *et al.* (2017) for homogenization of the nanocomposites in order to investigate the effects of using GPLs, as reinforcements in a nanocomposite, on the nonlinear bending responses of a beam. Also, a higher-order plate model is incorporated with the nonlinear theory of von-Kármán by some of the authors in order to consider for the impacts of thermal environment and elastic medium on the nonlinear bending and vibration characteristics of functionally graded graphene-reinforced composite (FG-

GRC) laminated plates (Shen *et al.* 2017a, Shen *et al.* 2017b). Also, the issue of postbuckling problem of a porous GPL reinforced (GPLR) nanocomposite beam is undertaken and studied by Barati and Zenkour (2017) with respect to the influences of geometrical imperfection. Yang *et al.* (2017) carried out an analysis on the stability of FG nanocomposite beams reinforced with GPLs. Also, Zhao *et al.* (2017) studied the bending and vibration behaviors of a FG trapezoidal plate reinforced with GPLs by employing the modified Halpin-Tsai model and the rule of mixture to predict the effective material properties. Besides, researchers have also probed the vibration, bending and compressive buckling of the GPLR polymeric nanocomposite plates via Mindlin-Reissner theory (Song *et al.* 2018). Graphene oxide also is a novel nanofiller with astounding thermal (Balandin *et al.* 2008), mechanical and optical properties (Yazid *et al.* 2018). In the recent years, it is found that graphene oxide can be a great reinforcement for the plates with polymer matrix in order to enhance the mechanical and functional properties of the polymer materials due to its remarkable compatibility with polymers (Potts *et al.* 2011). The experiments on this novel nanofiller show that monolayer GO has the Young modulus of 0.25 ± 0.15 TPa (Gómez-Navarro *et al.* 2008). Due to this fact, nanocomposites reinforced with GO have extraordinary tensile strength in addition to their low cost. GO has been also used in fabricating flexible displays and transparent conducting films, accumulators, and supercapacitors (Mikoushkin *et al.* 2011). Moreover, owing to the GOs' hierarchical structure, it can be utilized as an adsorbent material. Most recently, Zhang *et al.* (2018) surveyed the buckling, bending and vibration of the GOP reinforced (GOPR) nanocomposite beams via Timoshenko theory. Except the aforementioned paper, no other research can be found dealing with the mechanical behaviors of nanocomposite continuous systems reinforced with GOPs. To our best knowledge, the buckling problem of FG-GOPR nanocomposite plate, subjected to non-uniform magnetic field has never been studied up to now.

Present research is devoted to examining the influence of nonuniform magnetic field on the buckling responses of a GOPR nanocomposite beam. The material properties are achieved from Halpin-Tsai micromechanical scheme. Moreover, in the usage of Hamilton's principle, a refined higher-order beam model is implemented to reach the governing equations. Afterwards, Galerkin's method is implemented to solve the eigenvalue problem and compute the critical buckling load. Also, the accuracy of the method is verified too. Finally, the non-dimensional form of the results is presented for the sake of simplicity.

2. Theoretical formulations of the GOPRC beam for buckling analysis

2.1 Material homogenization

The structure of the beam, which is shown in Fig. 1, is consisted of an initial polymer matrix that is strengthened via a group of GOP fibers. The reinforcements are dispersed in the primary material via different patterns. These patterns



Fig. 1 Geometry of a composite beam

can be generated by putting the fibers in a series of specified positions which can be calculated by following simple modeling:

$$\begin{cases} V_{GOP} = V_{GOP}^* \text{GOPR-U} \\ V_{GOP} = \left(2 - 4 \frac{|z|}{h}\right) V_{GOP}^* \text{GOPR-O} \\ V_{GOP} = 4 \frac{|z|}{h} V_{GOP}^* \text{GOPR-X} \end{cases} \quad (1)$$

in which V_{GOP}^* is the volume fraction of GOPs and can be formulated as:

$$V_{GOP}^* = \frac{W_{GOP}}{W_{GOP} + \left(\frac{\rho_{GOP}}{\rho_M}\right) (1 - W_{GOP})} \quad (2)$$

where GOP and M subscripts are related to GOP reinforcements and the matrix, respectively. In addition, ρ stands for mass density and W_{GOP} denotes GOP weight fraction. Afterwards, it is necessary to earn the nanocomposite's equivalent elasticity modulus and Poisson's ratio. Herein, the Halpin-Tsai homogenization technique is extended for derivation of the material properties (Zhang *et al.* 2018). Now, the Young's modulus can be written as:

$$E_{eff} = 0.49E_l + 0.51E_t \quad (3)$$

where E_l and E_t account for longitudinal and transverse Young's modulus of the composite, respectively. These elastic parameters can be calculated as (Zhang *et al.* 2018):

$$E_l = \frac{1 + \xi_l \eta_l V_{GOP}}{1 - \eta_l V_{GOP}} \times E_M, E_t = \frac{1 + \xi_t \eta_t V_{GOP}}{1 - \eta_t V_{GOP}} \times E_M \quad (4)$$

where

$$\eta_l = \frac{\left(\frac{E_{GOP}}{E_M}\right) - 1}{\left(\frac{E_{GOP}}{E_M}\right) + \xi_l}, \eta_t = \frac{\left(\frac{E_{GOP}}{E_M}\right) - 1}{\left(\frac{E_{GOP}}{E_M}\right) + \xi_t} \quad (5)$$

in which E_{GOP} and E_M stand for GOPs and matrix Young modulus, respectively. Also, the geometry factors (ξ_l, ξ_t) are defined as follows (Zhang *et al.* 2018):

$$\xi_l = \xi_t = \frac{2d_{GOP}}{h_{GOP}} \quad (6)$$

In which the GOPs' diameter and thickness are shown with d_{GOP} and h_{GOP} respectively. Now, the effective Poisson's ratio of the composite can be achieved by using the rule of mixture in the following form:

$$\nu_{eff} = \nu_{GOP} V_{GOP} + \nu_M V_M \quad (7)$$

where V_{GOP} and V_M correspond with the volume fractions of GOPs and matrix, respectively. It should be mentioned that the effective mass density can be computed in the same form as Poisson's ratio is achieved in Eq. (7). The volume fractions are related to each other as:

$$V_{GOP} + V_M = 1 \quad (8)$$

2.2 Refined higher-order beam theory

The classical theory of beams and plates possesses some simplifying assumptions which leads to some limitations in modeling. For example, this theory cannot present reliable results whenever the slenderness and length-to-thickness ratios are inside 10. Due to this fact, the researchers have introduced some mathematical modeling which is able to estimate the shear stress and strain of the plates and beams (Fourn *et al.* 2018). Moreover, Bourada *et al.* (2019) employed sinusoidal shear deformation theory in order to investigate the dynamic behavior of the FG porous beam. In addition, She *et al.* (2017a) investigated the buckling and post-buckling analysis of the FG beams under thermal loadings by utilizing general higher-order shear deformation theory. In comparison to the other works in which the thickness stretching effect is taken into account (Bouafia *et al.* 2017) the very small difference was seen on the vibrational behavior of FG plates which could be negligible for the sake of simplicity. On the other hand, in some other researches, other versions of the classical kinematic theories are presented which are modified to be applicable in the cases that influences of the shear deformation cannot be ignored (Younsi *et al.* 2018). For the purpose of capturing the shear effect in the higher-order theorems, a shape function is presented in each theory. In this paper, the refined form of sinusoidal beam theory is utilized in order to achieve the kinematic relations of the beam. According to this theory, the displacement field of a beam can be written as:

$$u_x(x, z) = u(x) - z \frac{\partial w_b}{\partial x} - f(z) \frac{\partial w_s}{\partial x} \quad (9)$$

$$u_z(x, z) = w_b(x) + w_s(x) \quad (10)$$

where, u is longitudinal displacement and w_b , w_s are bending and shear deflections, respectively. The corresponding shape function of the employed theory is given as:

$$f(z) = z - \frac{h}{\pi} \sin\left(\frac{\pi z}{h}\right) \quad (11)$$

Now, the following equations indicate the nonzero strains of the beam:

$$\varepsilon_{xx} = \frac{\partial u}{\partial x} - z \frac{\partial^2 w_b}{\partial x^2} - f(z) \frac{\partial^2 w_s}{\partial x^2}, \gamma_{xz} = g(z) \frac{\partial w_s}{\partial x} \quad (12)$$

in which

$$g(z) = 1 - \frac{df(z)}{dz} \quad (13)$$

2.3 Hamilton's principle

Now, Hamilton's principle can be defined as:

$$\int_0^t \delta(U + V) dt = 0 \quad (14)$$

Here U is the variation of strain energy and V is work done by external forces, respectively. The virtual strain energy can be calculated as:

$$\delta U = \int_V (\sigma_{xx} \delta \varepsilon_{xx} + \sigma_{xz} \delta \gamma_{xz}) dV \quad (15)$$

Substituting Eqs. (9) – (13) in Eq. (15) yields:

$$\delta U = \int_0^L \left(N \frac{\partial \delta u}{\partial x} - M_b \frac{\partial^2 w_b}{\partial x^2} - M_s \frac{\partial^2 w_s}{\partial x^2} + Q \frac{\partial w_s}{\partial x} \right) dx \quad (16)$$

in which the stress resultants N , M_b , M_s , and Q can be written as:

$$[N, M_b, M_s] = \int_A [1, z, f(z)] \sigma_{xx} dA, \quad (17)$$

$$Q = \int_A g(z) \sigma_{xz} dA \quad (18)$$

Besides, in this research, the nanocomposite is assumed to be subjected to an in-plane magnetic field. Thus, the Maxwell's magnetic induction rules are extended to achieve the equivalent body force applied to the beam. Herein, the longitudinal magnetic field is:

$$H = (H_x, 0, 0), H_x = \bar{H}_x \sin\left(\frac{\pi x}{L}\right) \quad (19)$$

where \bar{H}_x is the amplitude of the longitudinal magnetic field. Maxwell's relation can be developed as:

$$\begin{aligned} f_z &= \eta \left[\nabla \times (\nabla \times (\vec{u} \times \vec{H})) \right] \vec{H} \\ &= \eta \left[H_x^2 \frac{\partial^2 (w_b + w_s)}{\partial x^2} + 2H_x \frac{\partial H_x}{\partial x} \frac{\partial (w_b + w_s)}{\partial x} \right. \\ &\quad \left. + H_x \frac{\partial^2 H_x}{\partial x^2} (w_b + w_s) \right] \end{aligned} \quad (20)$$

In which η is magnetic permeability and $\vec{u} = (u_x, 0, u_z)$ is displacement vector. By inserting the displacement field in above equation, the resultant Lorentz force can be achieved as:

$$\begin{aligned} f_{Lz} &= \int_A f_z dA = \psi_1 \frac{\partial^2 (w_b + w_s)}{\partial x^2} + \psi_2 \frac{\partial (w_b + w_s)}{\partial x} \\ &\quad - \psi_3 (w_b + w_s) \end{aligned} \quad (21)$$

where

$$\begin{aligned} \psi_1 &= \eta A \bar{H}_x^2 \sin^2\left(\frac{\pi x}{L}\right), \\ \psi_2 &= 2\eta A \left(\frac{\pi}{L}\right) \bar{H}_x^2 \sin\left(\frac{\pi x}{L}\right) \cos\left(\frac{\pi x}{L}\right), \\ \psi_3 &= \eta A \left(\frac{\pi}{L}\right)^2 \bar{H}_x^2 \sin^2\left(\frac{\pi x}{L}\right) \end{aligned} \quad (22)$$

Now, the variation of work done by external forces can be formulated as:

$$\delta V = \int_0^L \left(N_b \frac{\partial \delta(w_b + w_s)}{\partial x} \frac{\partial(w_b + w_s)}{\partial x} + \psi_1 \frac{\partial^2 \delta(w_b + w_s)}{\partial x^2} + \psi_2 \frac{\partial \delta(w_b + w_s)}{\partial x} - \psi_3 \delta(w_b + w_s) \right) dx \quad (23)$$

Therefore, once substituting Eqs. (16) and (23) in Eq. (14) and solving for the nontrivial response, the Euler-Lagrange equations of this problem are derived as:

$$\frac{\partial N}{\partial x} = 0, \quad (24)$$

$$\begin{aligned} \frac{\partial^2 M_b}{\partial x^2} - N_b \frac{\partial^2(w_b + w_s)}{\partial x^2} + \psi_1 \frac{\partial^2(w_b + w_s)}{\partial x^2} \\ + \psi_2 \frac{\partial(w_b + w_s)}{\partial x} - \psi_3(w_b + w_s) = 0, \end{aligned} \quad (25)$$

$$\begin{aligned} \frac{\partial^2 M_s}{\partial x^2} + \frac{\partial Q}{\partial x} - N_b \frac{\partial^2(w_b + w_s)}{\partial x^2} + \psi_1 \frac{\partial^2(w_b + w_s)}{\partial x^2} \\ + \psi_2 \frac{\partial(w_b + w_s)}{\partial x} - \psi_3(w_b + w_s) = 0 \end{aligned} \quad (26)$$

2.4 Constitutive equations

The constitutive equations of the nanocomposite structure including the stress-strain relations of isotropic materials are expressed as follows in order to obtain the fundamental elastic equations of solids.

$$\sigma_{ij} = C_{ijkl} \varepsilon_{kl} \quad (27)$$

where σ_{ij} and ε_{kl} are the constituents of second order stress and strain tensors, respectively; whereas, C_{ijkl} corresponds with the constituent of the fourth order elasticity tensor. Whenever extending the aforementioned equation for a shear deformable beam, the following relations can be reached:

$$\sigma_{xx} = E_{eff} \varepsilon_{xx}, \quad (28)$$

$$\sigma_{xz} = G_{eff} \gamma_{xz} \quad (29)$$

in which E_{eff} and G_{eff} signify the Young and shear moduli of the nanocomposite, respectively. Integrating from Eqs. (28) and (29) over the cross-section area of the beam, the following equations obtained for the stress resultants:

$$N = A \frac{\partial u}{\partial x} - B \frac{\partial^2 w_b}{\partial x^2} - B_s \frac{\partial^2 w_s}{\partial x^2}, \quad (30)$$

$$M_b = B \frac{\partial u}{\partial x} - D \frac{\partial^2 w_b}{\partial x^2} - D_s \frac{\partial^2 w_s}{\partial x^2}, \quad (31)$$

$$M_s = B_s \frac{\partial u}{\partial x} - D_s \frac{\partial^2 w_b}{\partial x^2} - H_s \frac{\partial^2 w_s}{\partial x^2}, \quad (32)$$

$$Q = A_s \frac{\partial w_s}{\partial x} \quad (33)$$

where

$$\begin{aligned} [A, B, D, B_s, D_s, H_s] \\ = \int_A [1, z, z^2, f(z), zf(z), f^2(z)] E_{eff} dA, \end{aligned} \quad (34)$$

$$A_s = \int_A g^2(z) G_{eff} dA \quad (35)$$

Now, inserting Eqs. (30) – (33) in Eqs. (24) – (26), the governing equations of GOPRC beams can be derived as follows:

$$A \frac{\partial^2 u}{\partial x^2} - B \frac{\partial^3 w_b}{\partial x^3} - B_s \frac{\partial^3 w_s}{\partial x^3} = 0, \quad (36)$$

$$\begin{aligned} B \frac{\partial^3 u}{\partial x^3} - D \frac{\partial^4 w_b}{\partial x^4} - D_s \frac{\partial^4 w_s}{\partial x^4} + N_b \frac{\partial^2(w_b + w_s)}{\partial x^2} \\ + \psi_1 \frac{\partial^2(w_b + w_s)}{\partial x^2} + \\ \psi_2 \frac{\partial(w_b + w_s)}{\partial x} - \psi_3(w_b + w_s) = 0, \end{aligned} \quad (37)$$

$$\begin{aligned} B_s \frac{\partial^3 u}{\partial x^3} - D_s \frac{\partial^4 w_b}{\partial x^4} - H_s \frac{\partial^4 w_s}{\partial x^4} + A_s \frac{\partial^2 w_s}{\partial x^2} \\ + N_b \frac{\partial^2(w_b + w_s)}{\partial x^2} \\ + \psi_1 \frac{\partial^2(w_b + w_s)}{\partial x^2} + \\ \psi_2 \frac{\partial(w_b + w_s)}{\partial x} - \psi_3(w_b + w_s) = 0 \end{aligned} \quad (38)$$

3. Solution procedure

Here, the Galerkin's method is applied to solve the governing equations based on refined higher order beam theory. Three kinds of boundary conditions such as simply supported-simply supported, simply supported-clamped and clamped-clamped are applied to the beam in the following form:

❖ Simply – supported (S):

$$w_b = w_s = N = M = 0 \text{ at } x = 0, L$$

❖ Clamped (C):

$$u = w_b = w_s = 0 \text{ at } x = 0, L$$

Now, following solutions can be applied for displacement fields for satisfying the above-mentioned boundary conditions:

$$u = \sum_{n=1}^{\infty} U_n \frac{\partial X_m(x)}{\partial x} \quad (39)$$

$$w_b = \sum_{n=1}^{\infty} W_{bn} X_m(x) \quad (40)$$

$$w_s = \sum_{n=1}^{\infty} W_{sn} X_m(x) \quad (41)$$

where U_n , W_{bn} , and W_{sn} are unknown Fourier coefficients. Once Eqs. (39) – (41) are inserted in Eqs. (36) – (38), the following relation can be obtained:

$$[K]_{3 \times 3} \begin{bmatrix} U_n \\ W_{bn} \\ W_{sn} \end{bmatrix} = 0 \tag{42}$$

in which K is stiffness matrix. The k_{ij} arrays can be calculated in the following form

$$\begin{aligned} k_{11} &= A \times \int_0^L \frac{\partial^3 X_m(x)}{\partial x^3} \frac{\partial X_m(x)}{\partial x} dx, k_{12} \\ &= -B \times \int_0^L \frac{\partial^3 X_m(x)}{\partial x^3} \frac{\partial X_m(x)}{\partial x} dx, \\ k_{13} &= -B_s \times \int_0^L \frac{\partial^3 X_m(x)}{\partial x^3} \frac{\partial X_m(x)}{\partial x} dx, k_{21} \\ &= -B \times \int_0^L \frac{\partial^4 X_m(x)}{\partial x^4} X_m(x) dx, \\ k_{22} &= -D \times \int_0^L \frac{\partial^4 X_m(x)}{\partial x^4} X_m(x) dx + \int_0^L \psi_1 \frac{\partial^2 X_m(x)}{\partial x^2} X_m(x) dx \\ &\quad + \int_0^L \psi_2 \frac{\partial X_m(x)}{\partial x} X_m(x) dx \\ &\quad - \int_0^L \psi_3 X_m(x) X_m(x) dx \\ &\quad - N^b \int_0^L \frac{\partial^2 X_m(x)}{\partial x^2} X_m(x) dx, \\ k_{23} &= -D_s \times \int_0^L \frac{\partial^4 X_m(x)}{\partial x^4} X_m(x) dx + \int_0^L \psi_1 \frac{\partial^2 X_m(x)}{\partial x^2} X_m(x) dx \\ &\quad + \int_0^L \psi_2 \frac{\partial X_m(x)}{\partial x} X_m(x) dx \\ &\quad - \int_0^L \psi_3 X_m(x) X_m(x) dx \\ &\quad - N^b \int_0^L \frac{\partial^2 X_m(x)}{\partial x^2} X_m(x) dx, \\ k_{31} &= -B_s \times \int_0^L \frac{\partial^4 X_m(x)}{\partial x^4} X_m(x) dx, \\ k_{32} &= -D_s \times \int_0^L \frac{\partial^4 X_m(x)}{\partial x^4} X_m(x) dx + \int_0^L \psi_1 \frac{\partial^2 X_m(x)}{\partial x^2} X_m(x) dx \\ &\quad + \int_0^L \psi_2 \frac{\partial X_m(x)}{\partial x} X_m(x) dx \\ &\quad - \int_0^L \psi_3 X_m(x) X_m(x) dx \\ &\quad - N^b \int_0^L \frac{\partial^2 X_m(x)}{\partial x^2} X_m(x) dx, \\ k_{33} &= -H_s \times \int_0^L \frac{\partial^4 X_m(x)}{\partial x^4} X_m(x) dx \\ &\quad + A_s \times \int_0^L \frac{\partial^2 X_m(x)}{\partial x^2} X_m(x) dx \\ &\quad + \int_0^L \psi_1 \frac{\partial^2 X_m(x)}{\partial x^2} X_m(x) dx \\ &\quad + \int_0^L \psi_2 \frac{\partial X_m(x)}{\partial x} X_m(x) dx \\ &\quad - \int_0^L \psi_3 X_m(x) X_m(x) dx - N^b \int_0^L \frac{\partial^2 X_m(x)}{\partial x^2} X_m(x) dx \end{aligned}$$

It shall be mentioned that the final form of X_m function for each boundary condition can be evaluated in the following form:

$$\begin{aligned} \text{S-S:} X_m &= \sin\left(\frac{n\pi x}{L}\right), \\ \text{C-S:} X_m &= \sin\left(\frac{n\pi x}{L}\right) \left[\cos\left(\frac{n\pi x}{L}\right) - 1\right], \\ \text{C-C:} X_m &= \sin^2\left(\frac{n\pi x}{L}\right) \end{aligned}$$

4. Numerical results and discussion

Herein, a detailed parametric study is performed to investigate the reinforcing influences of GOP on the buckling behavior of nanocomposite beams with various boundary conditions and distribution patterns of GOP. The material properties of the constituent materials are chosen as same as those presented by Zhang *et al.* (2018). Also, beam's thickness is supposed to be $h=5$ cm unless another value is mentioned. Moreover, magnetic permeability is $\eta=4\pi \times 10^{-7}$. Through this part, the influences of the different boundary condition will be figured out. Also, for the first time, the shear deformation effects on the buckling response of GOPRC beams are considered by implementing refined higher order beam theory. Accuracy of present model is verified, too. The natural frequencies of simply-supported (S-S) CNTRC beams are obtained via present model and compared with those of Zhang *et al.* (2018) and Wattanasakulpong and Ungbhakorn (2013). As can be observed, the results of present model correspond with those of published papers. In addition, the frequency values of present model are compared with the results reported by Zhang *et al.* (2018) and Wattanasakulpong and Ungbhakorn (2013) for GOPRC nanocomposite beams (Table 1, 2). In all the future results, the following dimensionless forms of buckling load and magnetic field intensity are used:

$$\Omega = \frac{N^b L^2}{E_{GOP} I}, H_0 = \frac{\eta A L^2}{E_{GOP} I} \bar{H}_x^2, I = \frac{bh^3}{12} \tag{43}$$

Table 1 Comparison of the first dimensionless frequency of S-S CNTRC beams ($L/h=15, V_{CNT}=0.12$)

Reference	Distribution type		
	UD	O	X
Wattanasakulpong and Ungbhakorn (2013)	0.9976	0.7628	1.1485
Zhang <i>et al.</i> (2018)	0.9842	0.7595	1.1249
Present model	0.9904	0.7528	1.1399

Table 2 Comparison of the first dimensionless frequency of S-S GOPRC beams ($W_{GOP} = 0.3\%$)

L/h		Distribution type		
		X-GOPRC	O-GOPRC	U-GOPRC
10	Zhang <i>et al.</i> (2018)	0.3379	0.2921	0.3159
	Present model	0.3576	0.3013	0.3095
15	Zhang <i>et al.</i> (2018)	0.2271	0.1959	0.2121
	Present model	0.2411	0.2009	0.2079
20	Zhang <i>et al.</i> (2018)	0.1708	0.1473	0.1595
	Present model	0.1815	0.1461	0.1564

Table 3 First ten dimensionless buckling loads of GOPRC beams for different distributions of the GOP and various magnetic field intensities with S-S edge condition ($L/h = 25$, $W_{GOP} = 1\%$)

n	$H_0=0.2$			$H_0=0.5$		
	GOPR-U	GOPR-X	GOPR-O	GOPR-U	GOPR-X	GOPR-O
1	0.36061	0.407339	0.31362	0.66061	0.707339	0.61362
2	0.759444	0.937722	0.575978	0.946944	1.125222	0.763478
3	1.509615	1.880636	1.112957	1.676281	2.047303	1.279624
4	2.523784	3.116036	1.856285	2.683159	3.275411	2.01566
5	3.751935	4.559437	2.778567	3.907935	4.715437	2.934567
6	5.144858	6.131742	3.853861	5.299025	6.285909	4.008028
7	6.65437	7.763368	5.055379	6.807432	7.916429	5.20844
8	8.235796	9.397928	6.356175	8.38814	9.550272	6.508519
9	9.849936	10.99331	7.730178	10.00179	11.14516	7.88203
10	11.46414	12.52068	9.153084	11.61564	12.67218	9.304584

Table 4 First ten dimensionless buckling loads of GOPRC beams for different distributions of the GOP and various magnetic field intensities with C-C edge condition ($L/h = 25$, $W_{GOP} = 1\%$)

n	$H_0=0.2$			$H_0=0.5$		
	GOPR-U	GOPR-X	GOPR-O	GOPR-U	GOPR-X	GOPR-O
1	0.859444	1.037722	0.675978	1.196944	1.375222	1.013478
2	2.536284	3.128536	1.868785	2.714409	3.306661	2.04691
3	5.150414	6.137298	3.859416	5.312914	6.299798	4.021916
4	8.238921	9.401053	6.3593	8.395953	9.558084	6.516332
5	11.46614	12.52268	9.155084	11.62064	12.67718	9.309584
6	14.59718	15.31101	12.06226	14.75031	15.46413	12.21539
7	17.49791	17.71548	14.93992	17.65021	17.86777	15.09222
8	20.11133	19.75866	17.69305	20.26309	19.91042	17.8448
9	22.42971	21.49169	20.2663	22.5811	21.64308	20.41769
10	24.47224	22.97096	22.63441	24.62337	23.12208	22.78554

First ten dimensionless buckling loads of GOPRC beams subjected to various magnetic field intensities with S-S boundary condition and different types of GOP distribution are tabulated in Table 3. By dividing the Table in two parts with respect to different magnetic field intensities, it is observed that first ten buckling loads become slightly higher as magnetic field intensity increases. Also, Table 3 shows that among these types of GOP distribution, the X-distribution leads to the strongest beams that can tolerate the highest buckling loads followed by the U-distribution and O-distribution. To investigate the influences of BCs on the variation of buckling loads, the results are classified in Table 4 by changing the BC to clamped-clamped (C-C) edge condition. It should be noted that except the effect of BC, all other effects that can be seen in Table 3 are preserved in Table 4, too. In this way, it can be found that applying the C-C BC leads to higher buckling loads in comparison with S-S one.

Fig. 2 depicts the effects of GOPs' weight fraction and different BCs on the variation of dimensionless buckling load of GOPRC beams neglecting the influences of magnetic field in a constant slenderness ratio. It can be seen that within each of these BCs, the dimensionless buckling

load of GOPRC beams increases greatly with an increment in the weight fraction of GOPs. Then, BCs' effects on the dimensionless stability response is investigated. As illustrated in Fig. 2, for the beams with C-C edge conditions, the improvement of dimensionless buckling load is remarkably higher than S-S and C-S BCs. Moreover, S-S BC has the lowest value of dimensionless buckling load. By considering same GOPs' weight fraction among these three boundary conditions shown in Fig. 2a, 2b and 2c, the largest dimensionless buckling load is about 70 for C-C BC while for the others it does not exceed 55.

Moreover, in Fig. 3, the effect of various magnetic field intensities on the first and second dimensionless buckling load of S-S beam with various GOPs' weight fraction are investigated. It can be found that the dimensionless buckling loads, with desirable GOPs' weight fraction, are increased linearly as magnetic field intensity is added. According to the figure, the dimensionless buckling loads become greater once the GOPs' weight fraction is increased. Besides, the increasing influence of nanoparticles which are utilized as reinforcements should be taken into account. In fact, the structure can be subjected to higher critical buckling loads whenever a greater amount of GOPs

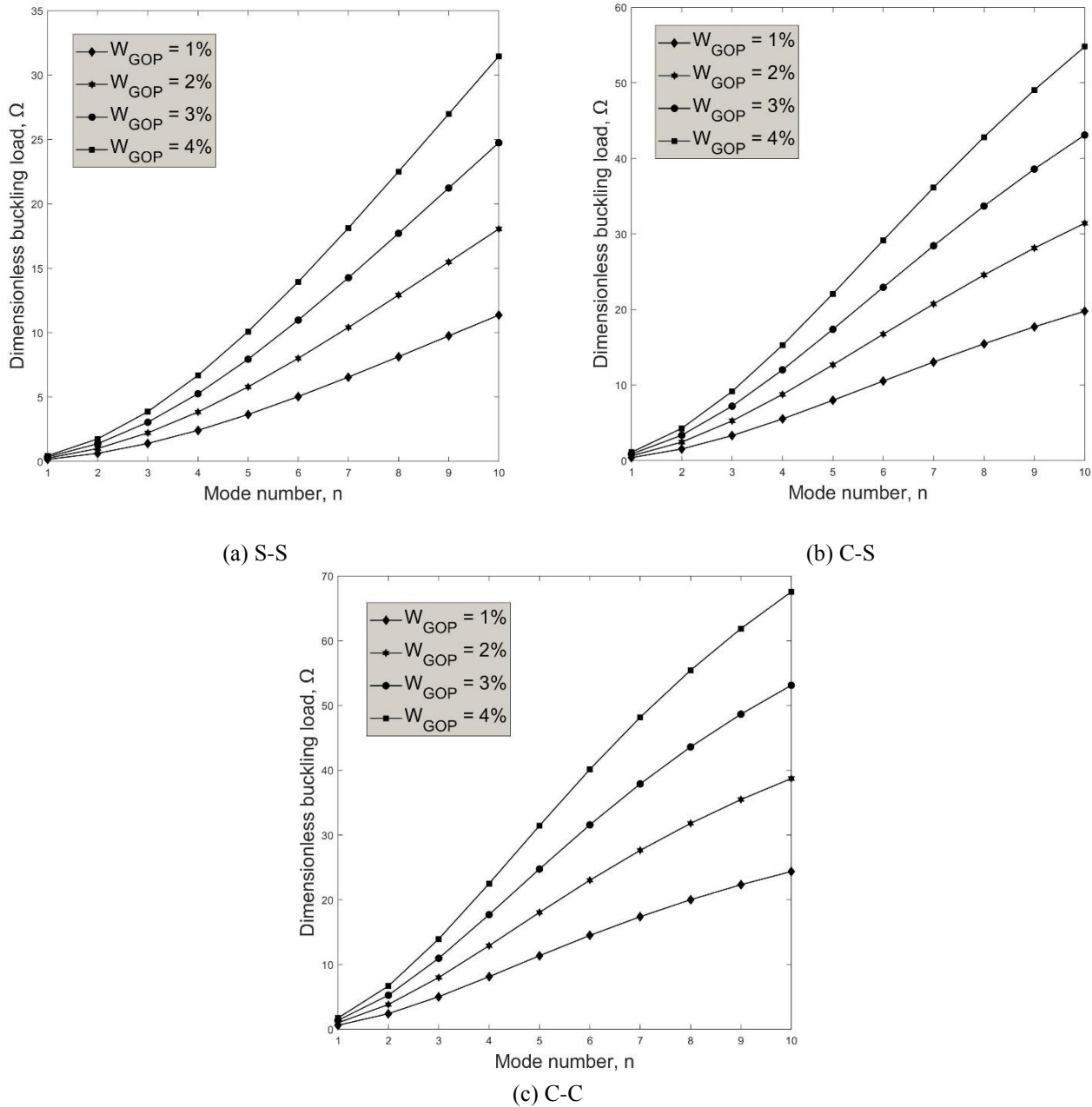


Fig. 2 Variation of the dimensionless buckling load of GOPRC beams versus mode number for various amounts of GOPs' weight fraction with respect to changes in edge conditions ($H_0 = 0, L/h = 25$)

is implemented. Naturally, a lower buckling load can be applied in the case of using pure epoxy. Also, changes in magnetic field intensity can affect the first mode's response more than the second mode's one.

At last, the variation of first dimensionless buckling load is plotted against GOPs' weight fraction by considering different values of slenderness ratio in Fig. 4. Actually, it can be found that the differences between the buckling load diagrams are negligible as GOPs' weight fraction is increased, hence, it can be figured out that slenderness ratio possesses less influence on the dimensionless buckling loads. Also, Fig. 4 show that the addition of GOP weight fraction causes linear increment in the amount of dimensionless buckling load.

5. Conclusion

In this study, buckling analysis of GOPRC beams under non-uniform magnetic field is conducted by using higher-order shear deformation theory. The beams are reinforced by various types of GOPs distributions along the thickness direction. By implementing Galerkin method, the governing differential equations are solved and also the accuracy of the numerical results are verified by comparison with some previous works. Finally, the influences of different parameters such as GOPs' weight fraction, magnetic field intensity, slenderness ratio and BCs on critical buckling load of GOPRC beams are investigated. Here the most important highlights of this study can be reviewed as follows:

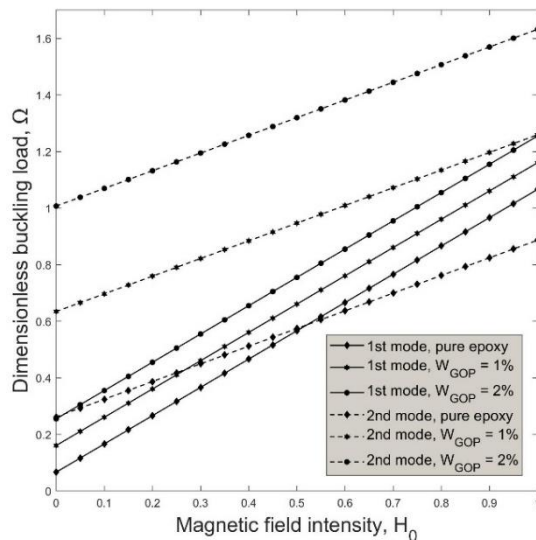


Fig. 3 Variation of the first and second dimensionless buckling load of S-S composite beams versus dimensionless magnetic field intensity for various amounts of GOPs' weight fraction and natural modes ($L/h = 25$)

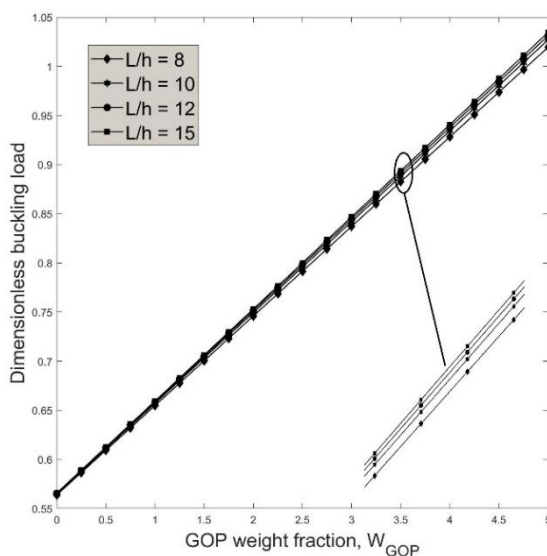


Fig. 4 Variation of the first dimensionless buckling load of S-S composite beams versus GOP weight fraction for various slenderness ratios ($H_0 = 0.5$)

- According to the results, it is figured out that the beam with X-distribution can tolerate higher buckling loads in comparison to the other distributions types which is meant that this beam is the strongest beam while, the beam with O-distribution is the weakest one.

- It was clearly seen that boundary conditions play an important role in changing the buckling loads in the way that C-C BC corresponds with the highest values of buckling loads and followed by C-S and S-S types.

- It is also revealed that buckling loads increase gradually as magnetic field intensity grows.

- It was observed that an increase in the GOPs' weight fraction can remarkably make the GOPRC beam structures to have a better buckling performances.

References

- Akgoz, B. and Civalek, O. (2013), "Buckling analysis of linearly tapered micro-columns based on strain gradient elasticity", *Struct. Eng. Mech.*, **48**, 195-205. <https://doi.org/10.12989/sem.2013.48.2.195>.
- Arani, A.G., Maghamikia, S., Mohammadimehr, M. and Arefmanesh, A. (2011), "Buckling analysis of laminated composite rectangular plates reinforced by SWCNTs using analytical and finite element methods", *J. Mech. Sci. Technol.*, **25**, 809-820. <https://doi.org/10.1007/s12206-011-0127-3>.
- Balandin, A.A., Ghosh, S., Bao, W., Calizo, I., Teweldebrhan, D., Miao, F. and Lau, C.N. (2008), "Superior thermal conductivity of single-layer graphene", *Nano Lett.*, **8**, 902-907. <https://doi.org/10.1021/nl0731872>.
- Barati, M.R. and Zenkour, A.M. (2017), "Post-buckling analysis of refined shear deformable graphene platelet reinforced beams with porosities and geometrical imperfection", *Compos. Struct.*, **181**, 194-202. <https://doi.org/10.1016/j.compstruct.2017.08.082>.
- Bouafia, K., Kaci, A., Houari, M.S.A., Benzair, A. and Tounsi, A. (2017), "A nonlocal quasi-3D theory for bending and free flexural vibration behaviors of functionally graded nanobeams", *Smart Struct. Syst.*, **19**, 115-126. <https://doi.org/10.12989/sss.2017.19.2.115>.
- Bourada, F., Bousahla, A.A., Bourada, M., Azzaz, A., Zinata, A. and Tounsi, A. (2019), "Dynamic investigation of porous functionally graded beam using a sinusoidal shear deformation theory", *Wind Struct.*, **28**, 19-30. <https://doi.org/10.12989/was.2019.28.1.019>.
- Ebrahimi, F. and Farazmandnia, N. (2017), "Thermo-mechanical vibration analysis of sandwich beams with functionally graded carbon nanotube-reinforced composite face sheets based on a higher-order shear deformation beam theory", *Mech. Adv. Mater. Struct.*, **24**, 820-829. <https://doi.org/10.1080/15376494.2016.1196786>.
- Ebrahimi, F. and Haghi, P. (2018), "A nonlocal strain gradient theory for scale-dependent wave dispersion analysis of rotating nanobeams considering physical field effects", *Coupled Syst. Mech.*, **7**, 373-393.
- Ebrahimi, F. and Rostami, P. (2018), "Wave propagation analysis of carbon nanotube reinforced composite beams", *Europ. Phys. J. Plus*, **133**, 285. <https://doi.org/10.1140/epjp/i2018-12069-y>.
- Ebrahimi, F. and Barati, M.R. (2016a), "Temperature distribution effects on buckling behavior of smart heterogeneous nanosize plates based on nonlocal four-variable refined plate theory", *J. Smart Nano Mater.*, **7**(3), 1-25. <https://doi.org/10.1080/19475411.2016.1223203>.
- Ebrahimi, F. and Barati, M.R. (2016b), "Vibration analysis of smart piezoelectrically actuated nanobeams subjected to magneto-electrical field in thermal environment", *J. Vib. Control*, <https://doi.org/10.1177/1077546316646239>.
- Ebrahimi, F. and Barati, M.R. (2016c), "Size-dependent thermal stability analysis of graded piezomagnetic nanoplates on elastic medium subjected to various thermal environments", *Appl. Phys. A*, **122**(10), 910. <https://doi.org/10.1007/s00339-016-0441-9>.
- Ebrahimi, F. and Barati, M.R. (2016d), "Static stability analysis of smart magneto-electro-elastic heterogeneous nanoplates embedded in an elastic medium based on a four-variable refined plate theory", *Smart Mater. Struct.*, **25**(10), <https://doi.org/10.1088/0964-1726/25/10/105014>.
- Ebrahimi, F. and Barati, M.R. (2016e), "Buckling analysis of piezoelectrically actuated smart nanoscale plates subjected to magnetic field", *J. Intelligent Mater. Syst. Struct.*, <https://doi.org/10.1177/1045389X16672569>.
- Ebrahimi, F., Barati, M.R. and Dabbagh, A. (2016), "A nonlocal strain gradient theory for wave propagation analysis in

- temperature-dependent inhomogeneous nanoplates”, *J. Eng. Sci.*, **107**, 169-182.
- Ebrahimi, F. and Dabbagh, A. (2016), “On flexural wave propagation responses of smart FG magneto-electro-elastic nanoplates via nonlocal strain gradient theory”, *Compos. Struct.*, **162**, <https://doi.org/10.1016/j.compstruct.2016.11.058>.
- Ebrahimi, F. and Hosseini, S.H.S. (2016a), “Thermal effects on nonlinear vibration behavior of viscoelastic nanosize plates”, *J. Thermal Stresses*, **39**(5), 606-625. <https://doi.org/10.1080/01495739.2016.1160684>.
- Ebrahimi, F. and Hosseini, S.H.S. (2016b), “Double nanoplate-based NEMS under hydrostatic and electrostatic actuations”, *Europe Phys. J. Plus*, **131**(5), 1-19. <https://doi.org/10.1140/epjp/i2016-16160-1>.
- Ebrahimi, F. and Barati, M.R. (2016f), “A nonlocal higher-order shear deformation beam theory for vibration analysis of size-dependent functionally graded nanobeams”, *Arabian J. Sci. Eng.*, **41**(5), 1679-1690. <https://doi.org/10.1007/s13369-015-1930-4>.
- Ebrahimi, F. and Barati, M.R. (2016g), “Vibration analysis of nonlocal beams made of functionally graded material in thermal environment”, *European Phys. J. Plus*, **131**(8), 279. <https://doi.org/10.1140/epjp/i2016-16279-y>.
- Ebrahimi, F. and Barati, M.R. (2016h), “Dynamic modeling of a thermo-piezo-electrically actuated nanosize beam subjected to a magnetic field”, *Appl. Phys. A*, **122**(4), 1-18. <https://doi.org/10.1007/s00339-016-0001-3>.
- Ebrahimi, F. and Barati, M.R. (2016i), “A unified formulation for dynamic analysis of nonlocal heterogeneous nanobeams in hygro-thermal environment”, *Appl. Phys. A*, **122**(9), 792. <https://doi.org/10.1007/s00339-016-0322-2>.
- Ebrahimi, F. and Barati, M.R. (2016j), “A nonlocal higher-order refined magneto-electro-viscoelastic beam model for dynamic analysis of smart nanostructures”, *J. Eng. Sci.*, **107**, 183-196. <https://doi.org/10.1016/j.ijengsci.2016.08.001>.
- Ebrahimi, F. and Barati, M.R. (2016k), “Hygrothermal effects on vibration characteristics of viscoelastic FG nanobeams based on nonlocal strain gradient theory”, *Compos. Struct.*, **159**, <https://doi.org/10.1016/j.compstruct.2016.09.092>.
- Ebrahimi, F. and Barati, M.R. (2016l), “Buckling analysis of nonlocal third-order shear deformable functionally graded piezoelectric nanobeams embedded in elastic medium”, *J. Brazilian Soc. Mech. Sci. Eng.*, **39**(3), 1-16.
- Ebrahimi, F. and Barati, M.R. (2016m), “Magnetic field effects on buckling behavior of smart size-dependent graded nanoscale beams”, *European Phys. J. Plus*, **131**(7), 1-14.
- Ebrahimi, F. and Barati, M.R. (2016n), “Buckling analysis of smart size-dependent higher order magneto-electro-thermo-elastic functionally graded nanosize beams”, *J. Mech.*, 1-11. <https://doi.org/10.1017/jmech.2016.46>.
- Feng, C., Kitipornchai, S. and Yang, J. (2017), “Nonlinear bending of polymer nanocomposite beams reinforced with non-uniformly distributed graphene platelets (GPLs)”, *Compos. Part B Eng.*, **110**, 132-140. <https://doi.org/10.1016/j.compositesb.2016.11.024>.
- Formica, G., Lacarbonara, W. and Alessi, R. (2010), “Vibrations of carbon nanotube-reinforced composites”, *J. Sound Vib.*, **329**, 1875-1889. <https://doi.org/10.1016/j.jsv.2009.11.020>.
- Fourn, H., Atmane, H.A., Bourada, M., Bousahla, A.A., Tounsi, A. and Mahmoud, S. (2018), “A novel four variable refined plate theory for wave propagation in functionally graded material plates”, *Steel Compos. Struct.*, **27**(1), 109-122. <https://doi.org/10.12989/scs.2018.27.1.109>.
- Gómez-Navarro, C., Burghard, M. and Kern, K. (2008), “Elastic properties of chemically derived single graphene sheets”, *Nano Lett.*, **8**, 2045-2049. <https://doi.org/10.1021/nl801384y>.
- Hamza-Cherif, R., Meradjah, M., Zidour, M., Tounsi, A., Belmahi, S. and Bensattalah, T. (2018), “Vibration analysis of nano beam using differential transform method including thermal effect”, *Adv. Nano Res.*, **54**, 1-14. <https://doi.org/10.4028/www.scientific.net/JNanoR.54.1>.
- Kant, T. and Babu, C. (2000), “Thermal buckling analysis of skew fibre-reinforced composite and sandwich plates using shear deformable finite element models”, *Compos. Struct.*, **49**(1), 77-85. [https://doi.org/10.1016/S0263-8223\(99\)00127-0](https://doi.org/10.1016/S0263-8223(99)00127-0).
- Lei, Z., Liew, K. and Yu, J. (2013), “Buckling analysis of functionally graded carbon nanotube-reinforced composite plates using the element-free kp-Ritz method”, *Compos. Struct.*, **98**, 160-168. <https://doi.org/10.1016/j.compstruct.2012.11.006>.
- Liew, K., Lei, Z., Yu, J. and Zhang, L. (2014), “Postbuckling of carbon nanotube-reinforced functionally graded cylindrical panels under axial compression using a meshless approach”, *Comput. Methods Appl. Mech. Eng.*, **268**, 1-17. <https://doi.org/10.1016/j.cma.2013.09.001>.
- Liu, G., Chen, X. and Reddy, J. (2002), “Buckling of symmetrically laminated composite plates using the element-free Galerkin method”, *J. Struct. Stability Dynam.*, **2**(3), 281-294. <https://doi.org/10.1142/S0219455402000634>.
- Mikoushkin, V., Shnitov, V., Nikonov, S.Y., Dideikin, A., Vul, A. Y., Sakseev, D., Vyalikh, D. and Vilkov, O.Y. (2011), “Controlling graphite oxide bandgap width by reduction in hydrogen”, *Tech. Phys. Lett.*, **37**, 942. <https://doi.org/10.1134/S1063785011100257>.
- Potts, J.R., Dreyer, D.R., Bielawski, C.W. and Ruoff, R.S. (2011), “Graphene-based polymer nanocomposites”, *Polymer*, **52**, 5-25. <https://doi.org/10.1016/j.polymer.2010.11.042>.
- Shan, L. and Qiao, P. (2005), “Flexural-torsional buckling of fiber-reinforced plastic composite open channel beams”, *Compos. Struct.*, **68**(2), 211-224. <https://doi.org/10.1016/j.compstruct.2004.03.015>.
- Shariyat, M. (2010), “A generalized global-local high-order theory for bending and vibration analyses of sandwich plates subjected to thermo-mechanical loads”, *J. Mech. Sci.*, **52**(3), 495-514. <https://doi.org/10.1016/j.ijmecsci.2009.11.010>.
- She, G.L., Yan, K.M., Zhang, Y.L., Liu, H.B. and Ren, Y.R. (2018a), “Wave propagation of functionally graded porous nanobeams based on non-local strain gradient theory”, *European Phys. J. Plus*, **133**, 368. <https://doi.org/10.1140/epjp/i2018-12196-5>.
- She, G.L., Yuan, F.G., Karami, B., Ren, Y.R. and Xiao, W.S. (2019), “On nonlinear bending behavior of FG porous curved nanotubes”, *J. Eng. Sci.*, **135**, 58-74. <https://doi.org/10.1016/j.ijengsci.2018.11.005>.
- She, G.L., Yuan, F.G. and Ren, Y.R. (2018b), “On wave propagation of porous nanotubes”, *J. Eng. Sci.*, **130**, 62-74. <https://doi.org/10.1016/j.ijengsci.2018.05.002>.
- She, G.L., Yuan, F.G., Ren, Y.R. and Xiao, W.S. (2017b), “On buckling and postbuckling behavior of nanotubes”, *J. Eng. Sci.*, **121**, 130-142. <https://doi.org/10.1016/j.ijengsci.2017.09.005>.
- Shen, H.S. and Xiang, Y. (2012), “Nonlinear vibration of nanotube-reinforced composite cylindrical shells in thermal environments”, *Comput. Methods Appl. Mech. Eng.*, **213**, 196-205. <https://doi.org/10.1016/j.cma.2011.11.025>.
- Shen, H.S., Xiang, Y. and Lin, F. (2017a), “Nonlinear bending of functionally graded graphene-reinforced composite laminated plates resting on elastic foundations in thermal environments”, *Compos. Struct.*, **170**, 80-90. <https://doi.org/10.1016/j.compstruct.2017.03.001>.
- Shen, H.S., Xiang, Y. and Lin, F. (2017b), “Nonlinear vibration of functionally graded graphene-reinforced composite laminated plates in thermal environments”, *Comput. Methods Appl. Mech. Eng.*, **319**, 175-193. <https://doi.org/10.1016/j.cma.2017.02.029>.
- Shen, H.S. and Zhang, C.L. (2010), “Thermal buckling and postbuckling behavior of functionally graded carbon nanotube-

- reinforced composite plates”, *Mater. Design*, **31**(7), 3403-3411. <https://doi.org/10.1016/j.matdes.2010.01.048>.
- Shojaee, S., Valizadeh, N., Izadpanah, E., Bui, T. and Vu, T.V. (2012), “Free vibration and buckling analysis of laminated composite plates using the NURBS-based isogeometric finite element method”, *Compos. Struct.*, **94**(5), 1677-1693. <https://doi.org/10.1016/j.compstruct.2012.01.012>.
- Sobhani, A., Saeedifar, M., Najafabadi, M.A., Fotouhi, M. and Zarouhas, D. (2018), “The study of buckling and post-buckling behavior of laminated composites consisting multiple delaminations using acoustic emission”, *Thin-Walled Struct.*, **127**, 145-156. <https://doi.org/10.1016/j.tws.2018.02.011>.
- Song, M., Yang, J. and Kitipornchai, S. (2018), “Bending and buckling analyses of functionally graded polymer composite plates reinforced with graphene nanoplatelets”, *Compos. Part B Eng.*, **134**, 106-113. <https://doi.org/10.1016/j.compositesb.2017.09.043>.
- Suk, J.W., Piner, R.D., An, J. and Ruoff, R.S. (2010), “Mechanical properties of monolayer graphene oxide”, *ACS nano*, **4**, 6557-6564. <https://doi.org/10.1021/nm101781v>.
- Tornabene, F., Fantuzzi, N., Viola, E. and Carrera, E. (2014), “Static analysis of doubly-curved anisotropic shells and panels using CUF approach, differential geometry and differential quadrature method”, *Compos. Struct.*, **107**, 675-697. <https://doi.org/10.1016/j.compstruct.2013.08.038>.
- Urthaler, Y. and Reddy, J. (2008), “A mixed finite element for the nonlinear bending analysis of laminated composite plates based on FSDT”, *Mech. Adv. Mater. Struct.*, **15**(5), 335-354. <https://doi.org/10.1080/15376490802045671>.
- Wang, Q., Shi, D., Liang, Q. and Pang, F. (2017), “Free vibrations of composite laminated doubly-curved shells and panels of revolution with general elastic restraints”, *Appl. Math. Model.*, **46**, 227-262. <https://doi.org/10.1016/j.apm.2017.01.070>.
- Wang, Z.X. and Shen, H.S. (2011), “Nonlinear vibration of nanotube-reinforced composite plates in thermal environments”, *Comput. Mater. Sci.*, **50**, 2319-2330. <https://doi.org/10.1016/j.commatsci.2011.03.005>.
- Wattanasakulpong, N. and Ungbhakorn, V. (2013), “Analytical solutions for bending, buckling and vibration responses of carbon nanotube-reinforced composite beams resting on elastic foundation”, *Comput. Mater. Sci.*, **71**, 201-208. <https://doi.org/10.1016/j.commatsci.2013.01.028>.
- Wu, H., Yang, J. and Kitipornchai, S. (2016), “Nonlinear vibration of functionally graded carbon nanotube-reinforced composite beams with geometric imperfections”, *Composites Part B Eng.*, **90**, 86-96. <https://doi.org/10.1016/j.compositesb.2015.12.007>.
- Yang, J., Wu, H. and Kitipornchai, S. (2017), “Buckling and postbuckling of functionally graded multilayer graphene platelet-reinforced composite beams”, *Compos. Struct.*, **161**, 111-118. <https://doi.org/10.1016/j.compstruct.2016.11.048>.
- Yas, M. and Samadi, N. (2012), “Free vibrations and buckling analysis of carbon nanotube-reinforced composite Timoshenko beams on elastic foundation”, *J. Pressure Vessels Piping*, **98**, 119-128. <https://doi.org/10.1016/j.ijpvp.2012.07.012>.
- Yazid, M., Heireche, H., Tounsi, A., Bousahla, A.A. and Houari, M. S. A. (2018), “A novel nonlocal refined plate theory for stability response of orthotropic single-layer graphene sheet resting on elastic medium”, *Smart Struct. Syst.*, **21**(1), 15-25. <https://doi.org/10.12989/sss.2018.21.1.015>.
- Younsi, A., Tounsi, A., Zaoui, F.Z., Bousahla, A.A. and Mahmoud, S. (2018), “Novel quasi-3D and 2D shear deformation theories for bending and free vibration analysis of FGM plates”, *Geomech. Eng.*, **14**(6), 519-532. <https://doi.org/10.12989/gae.2018.14.6.519>.
- Zhang, L., Lei, Z. and Liew, K. (2015), “Vibration characteristic of moderately thick functionally graded carbon nanotube reinforced composite skew plates”, *Compos. Struct.*, **122**, 172-183. <https://doi.org/10.1016/j.compstruct.2014.11.070>.
- Zhang, Z., Li, Y., Wu, H., Zhang, H., Wu, H., Jiang, S. and Chai, G. (2018), “Mechanical analysis of functionally graded graphene oxide-reinforced composite beams based on the first-order shear deformation theory”, *Mech. Adv. Mater. Struct.*, 1-9. <https://doi.org/10.1080/15376494.2018.1444216>.
- Zhao, Z., Feng, C., Wang, Y. and Yang, J. (2017), “Bending and vibration analysis of functionally graded trapezoidal nanocomposite plates reinforced with graphene nanoplatelets (GPLs)”, *Compos. Struct.*, **180**, 799-808. <https://doi.org/10.1016/j.compstruct.2017.08.044>.
- Zhen, W. and Wanji, C. (2006), “Free vibration of laminated composite and sandwich plates using global-local higher-order theory”, *J. Sound Vib.*, **298**(1-2), 333-349. <https://doi.org/10.1016/j.jsv.2006.05.022>.
- Zhu, P., Lei, Z. and Liew, K.M. (2012), “Static and free vibration analyses of carbon nanotube-reinforced composite plates using finite element method with first order shear deformation plate theory”, *Compos. Struct.*, **94**(4), 1450-1460. <https://doi.org/10.1016/j.compstruct.2011.11.010>.

CC